

# REPRODUCTION ANALYSIS FOR DEFORMATION BEHAVIOR OF ROCKFILL DAM UNDER CONSTRUCTION DURING LARGE EARTHQUAKE

S.Yoshida<sup>1</sup>  
H. Satoh<sup>2</sup>  
T. Sasaki<sup>3</sup>  
Y.Yamaguchi<sup>4</sup>

## ABSTRACT

During the Iwate-Miyagi Nairiku Earthquake in 2008, large settlement without sliding was observed at Isawa Dam, an earth core rockfill dam with a height of 132m then under construction in Iwate Prefecture, Japan. Dam height at the time of the earthquake was about 84m. In this study, we conducted reproduction analysis of deformation behaviour during the earthquake. For the analysis, we conducted dynamic laboratory tests of construction materials and evaluated differences of dynamic properties due to their saturated or unsaturated condition. We conducted the sliding deformation analysis using the Newmark method. We calculated settlement induced by the earthquake motion based on the cumulative damage theory and evaluated differences of behaviour due to their saturated or unsaturated condition. Reproducibility was confirmed by comparing analytical results and the observed differential settlement data. We found that the reproducibility of the shaking down settlement was fine in cases where the dynamic strength properties of saturated conditions in core material and those of unsaturated conditions in filter and rock materials were used. No sliding displacement was generated according to the sliding deformation analysis by the Newmark method. It was the same as the actual phenomenon of the dam during the earthquake.

## INTRODUCTION

Evaluation of the seismic safety of a dam is very important for dam risk management. According to “Guidelines for Seismic Performance Evaluation of Dams during Large Earthquakes (draft)” (MLIT, 2005) in Japan, the seismic safety of a rockfill dam is basically evaluated based on the sliding deformation caused by large earthquake motion. But the Iwate-Miyagi Nairiku Earthquake in 2008 caused relatively large-scale settlement without sliding at the Isawa Dam, a center earth-core type rockfill dam then under construction. In this paper, we conducted sliding deformation analysis. In addition, we conducted numerical analysis based on the cumulative damage theory using the dynamic strength test results of the dam body materials in saturated and unsaturated condition, and considered the effects of the dynamic strength properties on settlement behavior.

---

<sup>1</sup> NEWJEC Inc.(former Public Works Research Institute (PWRI)), Osaka City, Osaka Prefecture, Japan, yoshidast@newjec.co.jp.

<sup>2</sup> Public Works Research Institute (PWRI), Tsukuba City, Ibaraki Prefecture, Japan, sasaki@pwri.go.jp.

<sup>3</sup> Public Works Research Institute (PWRI), Tsukuba City, Ibaraki Prefecture, Japan, h-sato@pwri.go.jp.

<sup>4</sup> Japan Dam Engineering Center (JDEC), Tokyo, Japan, yamaguchi@jdec.or.jp

## OUTLINE OF THE ISAWA DAM

The Isawa Dam is a center earth-core type rockfill dam, with height of 132m, crest length of 723m, and dam volume of 13,500,000 m<sup>3</sup>, located about 10 km from the epicentre. Construction of the dam body had progressed 65.6% by volume on June 14, 2008 when the earthquake occurred. The typical cross-section of the Isawa Dam and the construction elevation at the time of the earthquake are shown in Figure 1. In the actual behavior of the dam body affected by the earthquake, a maximum of about 20 cm settlement occurred at the core part. Particularly, greater settlement was observed closer to the center of the embankment surface. Cracks parallel to the dam axis were also observed on the surface of the core and filter zones near the boundary of the two parts (Inabe, 2011). Cracks as wide as 10 to 20 cm were found on the filter zone surface. Figure 2 shows the appearance of cracks.

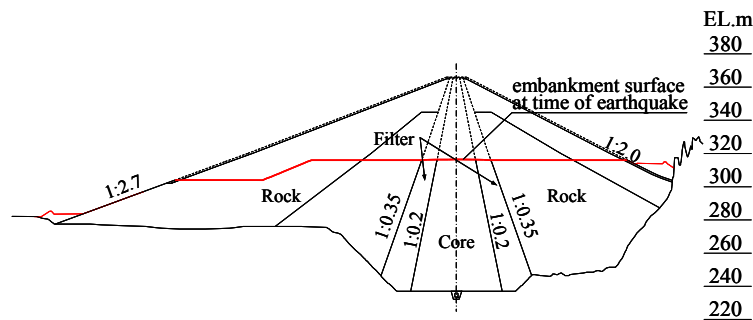


Figure 1. Standard cross-section of the Isawa Dam and construction elevation at the time of the earthquake

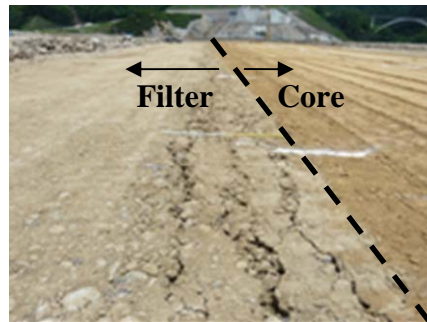


Figure 2. Cracks generated on the surface of the dam

## ANALYTICAL MODEL

The numerical analysis model used is a two-dimensional cross-section, which is a reproduction of the shape of the maximum cross-section with the amount of crown settlement by settlement gauge due to the earthquake.

In the embanking analysis, the dam body and foundation were modeled. In the dynamic analysis, only the dam body was modeled, and the bottom boundary of the dam body was regarded as the fixed boundary. Figure 3 shows the numerical analysis model of the dam body.

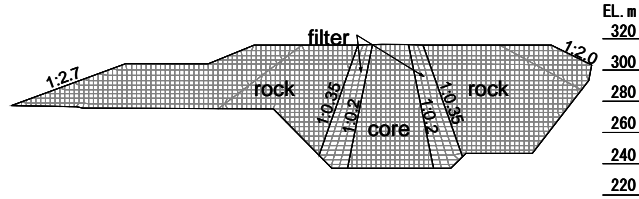


Figure 3. Numerical analysis model (dam body parts)

## PHYSICAL PROPERTIES FOR ANALYSIS

Physical properties used for analysis are determined by the design values and laboratory test results of the Isawa Dam.

### Physical properties in dynamic analysis

Material physical properties used in dynamic analysis are shown in Table 1. For the initial shear modulus and strain dependency characteristics, laboratory tests conducted both in saturated and unsaturated condition, but the test results in all zones under the unsaturated condition were used for this study. The strain dependency characteristics of dam materials are shown in Figure 4. Because only the dam body was modeled in the dynamic response analysis, 15% radiation damping ratio was added to the material damping ratio as the energy dissipation effect through the foundation.

Table 1. Physical properties in dynamic response analysis

Zone	Saturated condition	Initial shear modulus $G_0$ (MPa) <sup>*1)</sup>	Strain dependency characteristics <sup>*2)</sup>		Poisson ratio $\nu$ <sup>*3)</sup>
			$\gamma_r$	$h_{max}$ (%)	
Core	Unsaturated	$294.879\sigma_m^{0.444}$	$1.06 \times 10^{-3}$	18.0	Sawada's formula
Filter	Unsaturated	$628.347\sigma_m^{0.665}$	$4.74 \times 10^{-4}$	15.6	
Rock	Unsaturated	$737.070\sigma_m^{0.680}$	$4.80 \times 10^{-4}$	14.0	

\*1)  $\sigma_m'$ : Average effective stress after embanking analysis  $\sigma_m' = (1+\nu) \cdot (\sigma_1 + \sigma_3) / 3$

\*2)  $G/G_0 = 1 / (1 + \gamma / \gamma_r)$ ,  $h = h_{max} (1 - G/G_0)$

\*3)  $\nu = 0.450 - 0.006Z^{0.60}$  [core material]

$\nu = 0.375 - 0.006Z^{0.58}$  [filter and rock materials (shallower than the phreatic surface)]

$\nu = 0.490 - 0.001Z^{0.95}$  [filter and rock materials (deeper than the phreatic surface)]

Z: depth from the surface of the dam body (m)

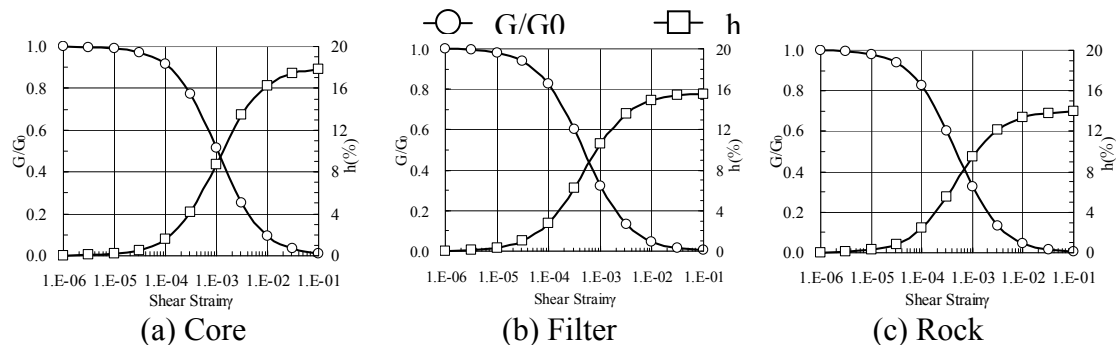


Figure 4. Strain dependency of shear modulus and material damping ratios

## Physical properties in cumulative damage theory analysis

The cumulative strain characteristics for each material were set based on the results of cyclic triaxial tests. Figure 5 shows the cumulative strain characteristics for each material under the saturated and unsaturated conditions. But, because the cyclic triaxial test for filter material was not carried out under unsaturated condition, we can not create the cumulative strain curve of the filter material under unsaturated condition. Therefore, the cumulative strain characteristics of the filter material under unsaturated condition were estimated by multiplying the cumulative strain ratio of the rock material and the filter material in the saturated condition by the cumulative strain of the unsaturated rock material. One of the features for all materials is that strains were much smaller in the unsaturated condition than in the saturated condition. Table. 2 shows the regression approximation equations of cumulative strain characteristics.

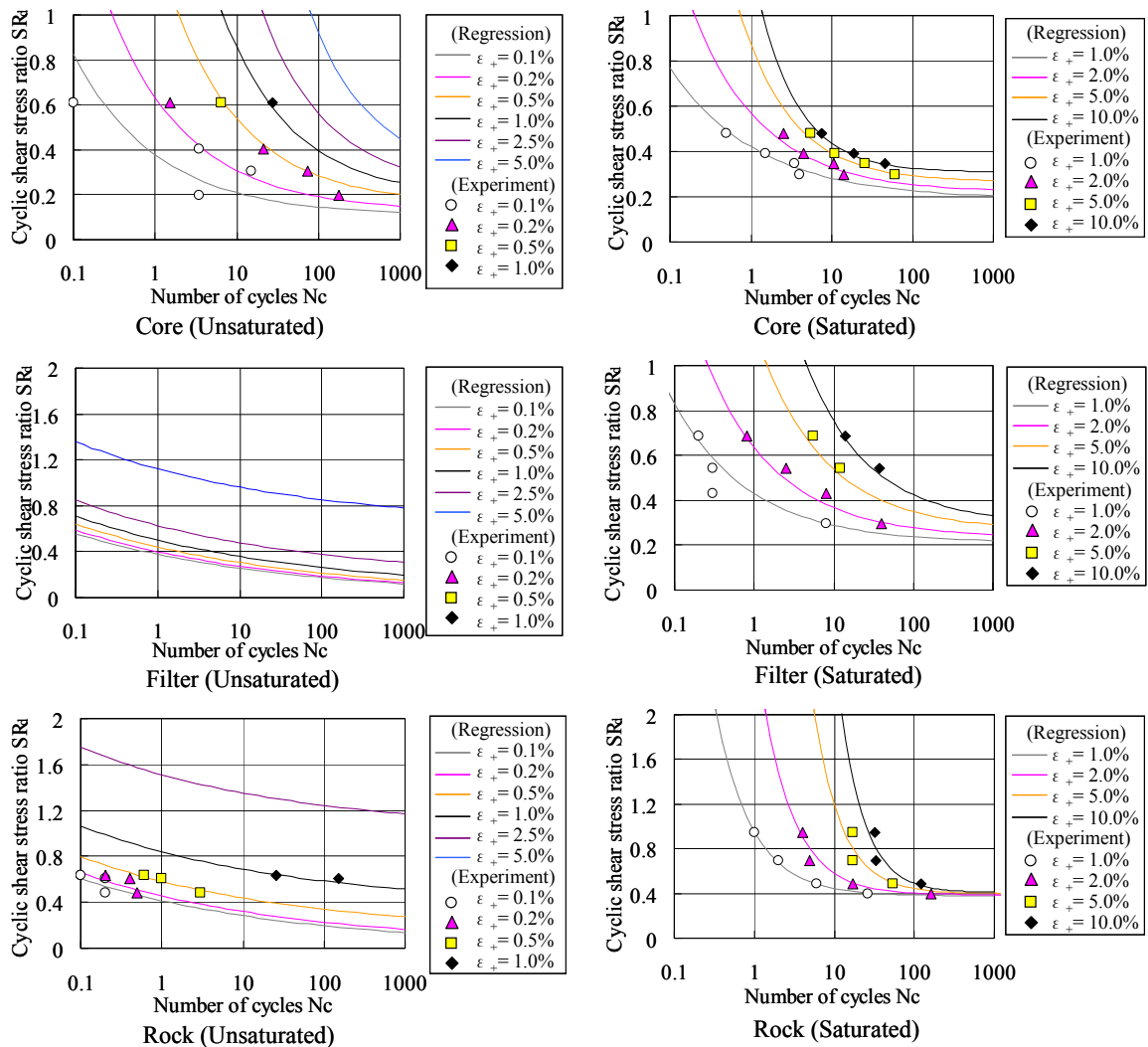


Figure 5. Cumulative strain characteristics

Table 2. Regression approximation equations of cumulative strain characteristics

Zone	Saturated condition	$SR_d \sim N_c$ regression approximation equations
Core	Unsaturated	$SR_d = 2.15 \varepsilon^{0.90} \cdot N_c^{(-0.51 \varepsilon^{0.08})} + 0.19 \varepsilon^{0.25}$
	Saturated	$SR_d = 0.23 \varepsilon^{0.60} \cdot N_c^{(-0.40 \varepsilon^{0.33})} + 0.19 \varepsilon^{0.21}$
Filter	Unsaturated	$SR_d = 0.44 \varepsilon^{0.07} \cdot N_c^{-0.17} + 0.06 \varepsilon^{1.46}$
	Saturated	$SR_d = 0.22 \varepsilon^{0.87} \cdot N_c^{(-0.45 \varepsilon^{0.09})} + 0.21 \varepsilon^{0.15}$
Rock	Unsaturated	$SR_d = 0.47 \varepsilon^{0.07} \cdot N_c^{-0.17} + 0.37 \varepsilon^{1.46}$
	Saturated	$SR_d = 0.57 \varepsilon^{2.01} \cdot N_c^{(-0.96 \varepsilon^{0.17})} + 0.38 \varepsilon^{0.03}$

\*)  $SR_d$ : cyclic shear stress ratio;  $N_c$ : repeated times,  
 $\varepsilon$ : cumulative axial strain (%)

### INPUT SEISMIC MOTIONS

Because no seismographs were installed at the Isawa Dam during the Iwate-Miyagi Nairiku Earthquake in 2008, no seismic motions were recorded at the site. Therefore, input seismic motions used for the seismic response analysis were estimated acceleration time records at the foundation of an existing rockfill dam located only about 2 km away from the Isawa Dam (Mitsuishi, 2008). The input seismic motions that were used are shown in Figure 6.

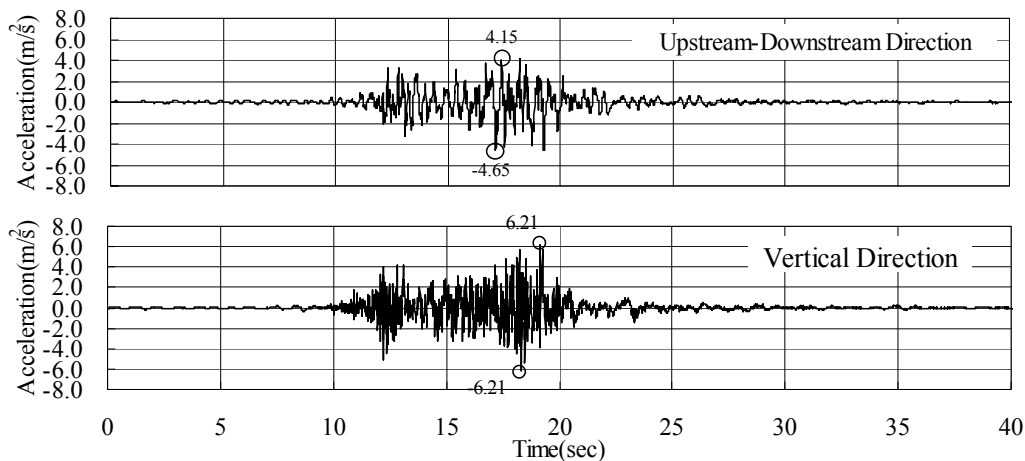


Figure 6. Input seismic motions (Mitsuishi, 2008)

### RESULTS OF STATIC AND SEISMIC RESPONSE ANALYSIS

Figure 7 shows the initial shear modulus  $G_0$  and convergent shear modulus  $G$  in the equivalent linearization analysis.  $G_0$  and  $G$  increase as the depth from the surface of the dam body increases.  $G_0$  is smaller in the core zone than in other zones because of so-called “arch action”. Figure 8 shows the vertical distributions of the maximum accelerations in the horizontal direction. The response acceleration increases near the surface of the dam body where  $G_0$  and  $G$  are smaller, and the accelerations at the dam

crest are 4.66 to 5.92 m/s<sup>2</sup> relative to the input maximum acceleration of 4.65m/s<sup>2</sup>. The response amplification ratio obtained was about 1.0 to 1.3.

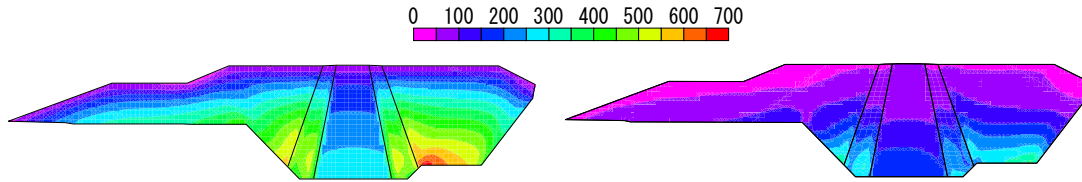


Figure 7. Distribution of initial and convergent shear modulus (unit: MPa)

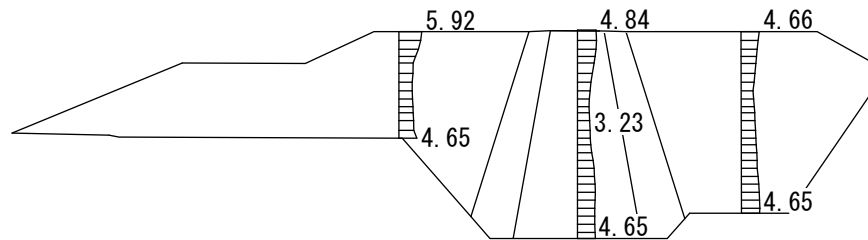


Figure 8. Maximum acceleration distributions in the upstream and downstream direction (unit: m/s<sup>2</sup>)

### SLIDING DEFORMATION ANALYSIS

Based on visual inspection just after the Iwate-Miyagi Nairiku Earthquake in 2008, no sliding deformation was observed at the Isawa Dam. For sliding deformation analysis in our research, the time histories of the average response accelerations of the slip circles were calculated from the seismic response analysis results, and the sliding deformation was calculated using the Newmark method (Tateyama, 1998), (RTRI, 1999), (Yamaguchi, 2005).

#### Analytical method

Shear strength used in sliding deformation analysis was determined based on the design values and triaxial compression test values using the following equations shown in Table 3.

< Seismic coefficient method (C  $\phi$  method) >

$$\tau_f = \sigma_n \cdot \tan \phi + C \quad (1)$$

< Modified seismic coefficient method (Ab method) >

$$\tau_f = A \cdot \sigma_n^b \quad (2)$$

where  $\tau_f$  is shear strength ( $\text{N/mm}^2$ ),  $\sigma_n$  is normal stress ( $\text{N/mm}^2$ ),  $\phi$  is internal friction angle ( $^\circ$ ) and  $C$  is cohesion ( $\text{N/mm}^2$ ). For the slip circles used in sliding deformation analysis, a total of seven circles on the upstream side are used as shown in Figure 9.

### Analytical results

The results of the sliding deformation analysis conducted using the Newmark method are shown in Table 4. All circles have safety factors higher than 1.0, which indicate the results of no occurrence of sliding and agree with the actual phenomena. As  $y/H$  or  $x/L$  increases, the safety factor decreases. The minimum safety factor is 2.285 in No. 5 circle.

Table 3. Shear strength constants used in sliding analysis

Zone	C, $\phi$ method		Ab method (MPa)	
	C	$\phi$ ( $^\circ$ )	A	b
Rock	—	—	0.977	0.827
Filter	—	—	1.322	0.902
Core	0.0	36.0	—	—

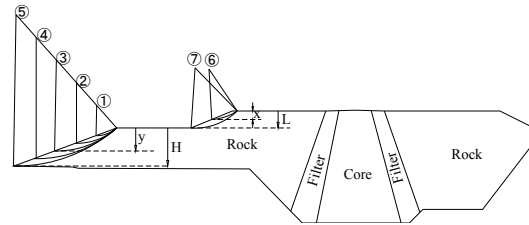


Figure 9. Considered slip circles

Table 4. Sliding deformation analysis results

Circle No.	Radius R(m)	y/H (x/L)	Dynamic analysis		Sliding analysis
			Maximum acceleration	Occurrence time	Minimum safety factor
			( $\text{m/s}^2$ )	(sec)	Fs
①	21.38	0.2	0.594	17.54	4.164
②	42.76	0.4	0.481	17.51	2.953
③	64.15	0.6	0.381	17.49	2.644
④	85.53	0.8	0.313	17.46	2.518
⑤	106.67	1.0	0.302	13.66	2.285
⑥	35.64	0.5	0.433	17.64	4.022
⑦	42.55	1.0	0.306	17.63	2.937

## REPRODUCTION ANALYSIS USING CUMULATIVE DAMAGE THEORY

### Analytical method

In the analytical method used here, the static stress distribution within the dam body was calculated by static analysis considering embanking processes. Seismic response analysis using initial stresses by static analysis was conducted to calculate the seismic response in the dam body. As for the embanking analysis, the nonlinear elastic analysis considering the embanking process based on the Duncan-Chang model was employed. In the seismic response analysis, the complex response analysis based on the equivalent linearization method was adopted. As for the cumulative damage theory analysis, it was conducted based on the concept that a permanent displacement of embankment materials caused by

an earthquake can be produced by the effects of cyclic loading (Shimamoto, 2008). Figure 10 shows the cumulative damage theory analysis flow. Cyclic shear stress ratio  $SR_d$  in cumulative damage theory analysis is calculated by the following equation in this study.

$$SR_d = \{(\sigma_{1d} - \sigma_{3d})/2\}/\sigma'_m \quad (3)$$

Where  $\sigma_{1d}$  and  $\sigma_{3d}$  are incremental stress by seismic response analysis and  $\sigma'_m$ 's mean effective stress in static analysis.

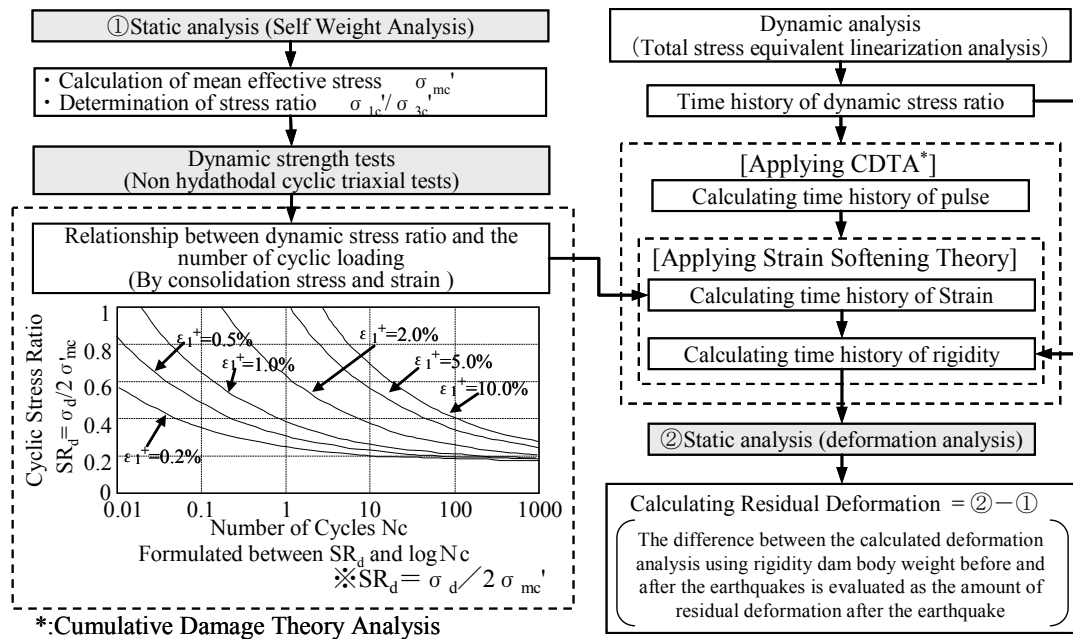


Figure 10. Cumulative damage theory analysis flow

### Analytical results

Figure 11 shows the permanent deformation in all three cases, and Figure 12 the vertical distributions of settlement. For Case 1 in which the physical properties in the unsaturated condition are applied to all materials, shear modulus reduction is small in the core zone, the settlement distribution did not agree with the measured value by the differential settlement gauge installed in the dam body, and was also different from the measurement result of largest settlement at the core part. On the other hand, the shear modulus dropped greatly in all zones in Case 2 where the saturated condition is applied to all materials, and the calculated settlement became greater than the actual measurement values in all zones. Because strain increases in the saturated condition in the rock zone, large settlement occurred in the rock zone. This is expected considering the tendency of the cumulative strain characteristics. Furthermore, it is presumed that as great settlement occurred in the rock zone, the filter and core zones also followed it, resulting in greater settlement. When compared with the measured values, the calculated values turned out to be greater than



the measured values in all zones. In Case 3 where the saturated condition only applies to the core material, the calculated values agreed with the measured values with relatively high precision although a slight difference with the measurement was observed in the downstream rock zone. Because the rapid rise of pore pressures in the core zone was observed by the pore pressure gauges during the earthquake at the Isawa Dam (Inabe, 2008), it is considered to have been in a state close to saturation conditions in core zone. The good reproducibility is understood to be obtained for Case 3 from such phenomena about the pore pressure because real conditions regarding saturation were reflected in the analysis.

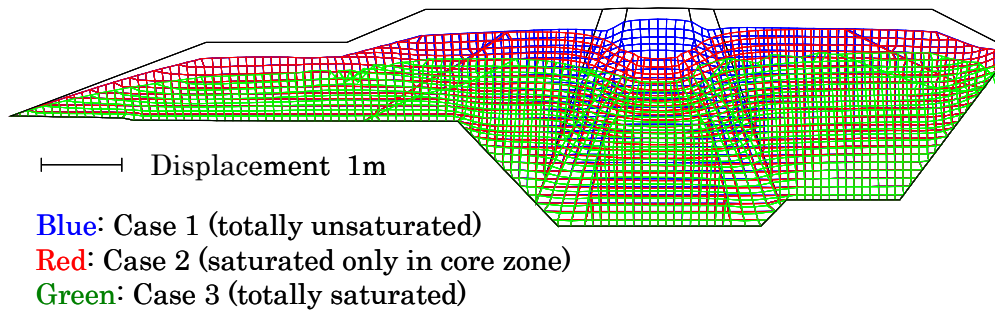


Figure 11. Residual deformation by cumulative damage theory analysis

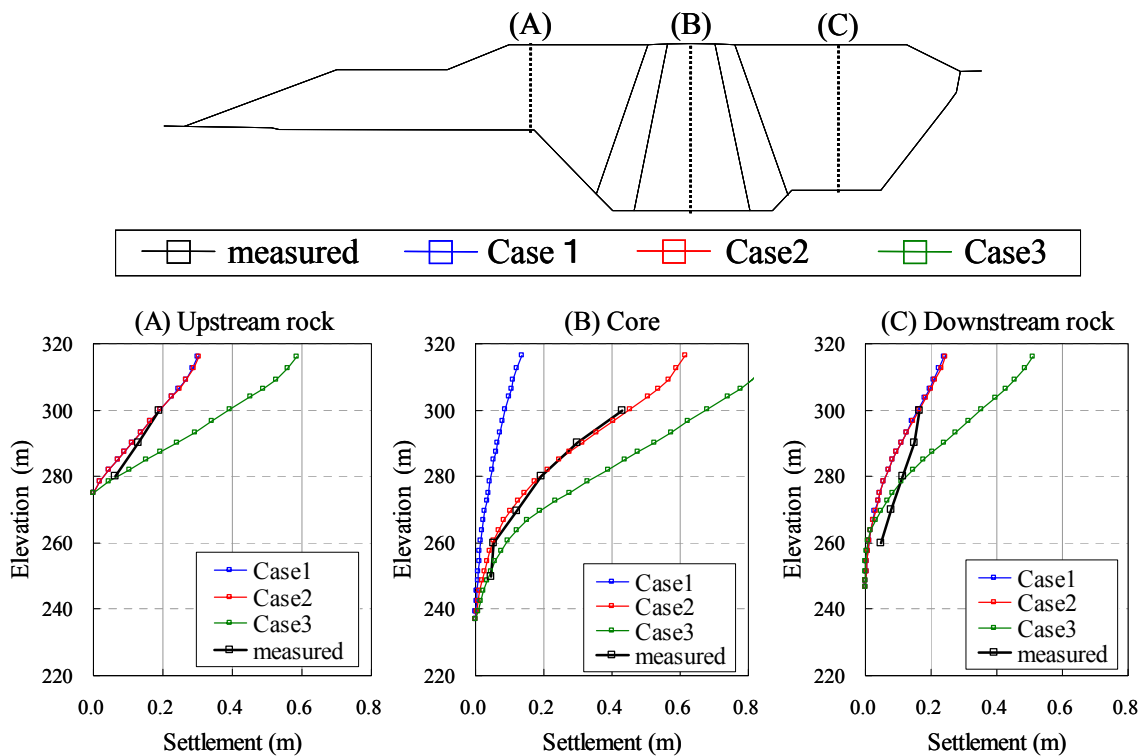


Figure 12. Comparison between the measured settlement and the analytical results

## CONCLUSIONS

In this paper, we conducted reproduction analysis of deformation behavior of a rockfill dam where settlement without sliding occurred during the Iwate-Miyagi Nairiku Earthquake in 2008. We successfully reproduced the settlement behavior of the dam affected by the earthquake using cumulative damage theory analysis. Reproduction analysis results agreed well with the observed results when the saturated condition was applied as the cumulative strain characteristic only for the core material. Sliding deformation analysis using the Newmark method resulted in the smallest safety ratio of 2.285 and therefore no sliding was produced. In conclusion, it is definitely considered that the shaking down settlement of the sample dam in this study due to the earthquake was well reproduced by the combination of the numerical analysis method and the techniques used to set material properties shown in this paper.

## REFERENCES

Inabe, S, Sakakibara, J, 2011, Occurrence of Core Cracking of the Isawa Dam Body by the 2008 Iwate-Miyagi Nairiku Earthquake, Engineering for Dams, No. 292, pp.54-63 (in Japanese)

Mitsubishi, S, Otani, T, et al., 2008, Report on Damage to Infrastructures and Buildings by the 2008 Iwate-Miyagi Nairiku Earthquake, Technical Note of Public Works Research Institute, No.4120, pp.90-137

River Bureau, Ministry of Land, Infrastructure, Transport and Tourism (MLIT), 2005, Guidelines for Seismic Performance Evaluation of Dams During Large Earthquakes (Draft). (in Japanese)

Shimamoto, K., Yasuda, N., Yamaguchi, Y., and Sato, H, 2008 Evaluation of Earthquake-Induced Deformation of Embankment Dams Using Cumulative Damage Theory, Proc. ICOLD 76th Annual Meeting

Tateyama, M, Tatsuoka, F, Koseki, J, Horii, K, 1998, Studies on Seismic Design Method for Soil Structures, Railway Technical Research Institute Report, Vol.12, No.4, pp.7-12  
Railway Technical Research Institute, 1999, Design Standards for Railway Structures and Commentary (Maruzen Co), pp.317-329

Yamaguchi, Y, Tomida, N, Mizuhara, M, 2005, Study on Earthquake-induced Sliding Deformation of Rockfill Dams, Journal of Japan Society of Dam Engineers, Vol.15, No.2, pp.120-136